L-wave generation is described in a few papers (Ref 4, 5, 8, 45).

Angle-Beam and Shear-Horizontal Plate Modes Generated Using the Periodic Permanent Magnet EMAT Structure. The PPM structure shown in Fig. 7 may be used to generate SH-waves that propagate either parallel to or at any angle with respect to the metal surface. (The conversion efficiency gradually decreases to zero as the beam angle, with respect to the metal surface, approaches 90°; the beam angle is determined by the PM periodicity and the frequency of the T-coil current.) When used with material less than a few wavelengths in thickness, the periodic permanent magnet EMAT structure generates SH-guided-wave modes that propagate with a velocity that can depend on both the mode frequency and the material thickness. Except for the SH_o mode, SH-guided modes are dispersive, meaning they travel at a velocity that depends on both the SH-mode frequency and the material thickness. A more extensive discussion of guided-mode dispersion is given in the section "Non-Shear-Horizontal Guided-Wave (Plate and Pipe) Modes" in this article as part of discussions of other types of guided-wave modes. The SH-dispersion curves also are given there.

Although this structure can be used with magnetic metals, several complications are commonly encountered; the most significant one is generating a lot of noise when such a structure is moved over the surface. The section "Special Considerations for Using EMATs with Magnetic Materials" in this article describes an alternative means of generating SH-waves in materials that exhibit MS; typically, this approach uses a PEM that avoids most of the magnetic noise issues mentioned earlier. The section also discusses other applications of PEMs.

Angle-Beam, Shear-Vertical, and Angle-Beam L-Wave Meander Coil EMATs. One common use of meander coil EMATs is for generating angle-beam SV-waves. Angle-beam L-waves also may be generated using MCs, but the conversion efficiency is lower than for SV-waves by approximately a factor of 4. The beam angle is determined by the T-coil current frequency and the MC period. As shown in Fig. 8, there is a small dependence of the beam angle on whether the bias field is perpendicular or parallel to the metal surface. If the bias field is at an angle with respect to the surface, then each component is separately responsible for generating an angle-beam wave. The insertion loss dependence on bias field orientation is related to the direction of the Lorentz driving force. Also clear in Fig. 8 is that both SV- and L-waves have an insertion loss that depends very strongly on the beam angle; this angle dependence is determined by the material Poisson's ratio. For SV-waves, the insertion loss is lowest at approximately 37 to 40°, while for L-waves, the insertion loss is lowest in the range of 45 to 65°. The precise angle dependence of insertion loss for SV- and L-waves for 6061 aluminum alloy (Poisson's ratio of 0.33) for the bias field perpendicular and parallel to the induced current direction is shown in Fig. 8.

Surface Waves Generated Using Meander Coils. Surface or Rayleigh waves (R-waves) are the limiting case of plate waves where the plate thickness becomes very large when compared to the propagating wavelength, which, for R-waves, is defined by the MC period. The MC configuration shown in Fig. 4(c) may be used for generating and receiving R-waves with the bias field at any angle with respect to the metal surface. If one wishes to use the field-parallel case, then a PEM often is the best choice for providing the bias field. The Poisson's ratio governs the coupling of surface traction to R-wave displacements.

Non-Shear-Horizontal Guided-Wave (Plate and Pipe) Modes. An MC or versions thereof

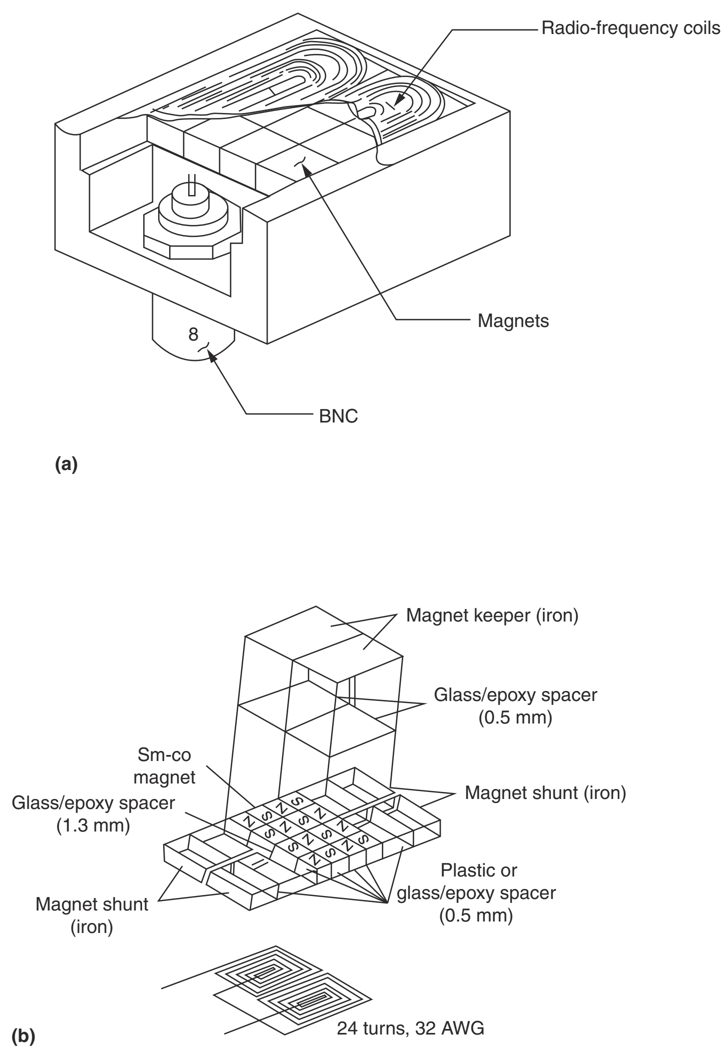

Fig. 7 (a) Cutaway view of a general but practical periodic permanent magnetic (PPM) electromagnetic acoustic transducer (EMAT) structure. (b) Exploded view of a periodic permanent magnet EMAT that has good rejection of common-mode electrical pickup. For most periodic permanent magnet EMAT applications, attention must be given to the size and location of magnet shunts, magnet keepers (backing iron), and nonmagnetic spacers between the PPMs. Generally, enclosures are made of aluminum or soft brass. Adapted from Ref 18. Also see Ref 6–8 and 22 for additional information on shear-horizontal EMAT use and construction.

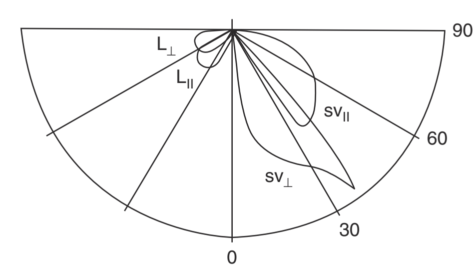

Fig. 8 Relative efficiency for generating angle-beam shear-vertical (SV) and longitudinal (L) waves for cases of the magnetic field parallel and perpendicular to the surface of a nonmagnetic metal. The case illustrated is for aluminum with Poisson's ratio of 0.33, but most metals except beryllium exhibit similar results.

placed in a B-field at any angle with respect to the metal surface also can be used to generate a variety of guided-wave modes in plates, pipes, strips, rods, and similar two-dimensional structures. This article uses the term *guided waves* to refer to any elastic mode that propagates in a material of finite dimension in the direction generally perpendicular to the propagation direction; included are such terms as rod waves, plate waves, and Lamb waves. The guided-mode wavelength is determined by several factors, including material properties, material dimensions, the exciting transducer, and its excitation frequency. The relationship is complex but the use of dispersion curves allows one to determine group and phase velocities when the frequency, MC period, material properties, and dimensions are known. The MC and magnet structure used to generate these modes are similar to the ones shown in Fig. 4(c) and Fig. 9 for generating surface waves and angle-beam SV- and L-waves. However, in many applications, the physical size of guided-wave EMATs is much larger than for the other wave modes due to the longer wavelengths that frequently are employed in UNDE applications.

These guided-wave modes, similar to the SH-guided modes mentioned in the section "Angle-Beam and Shear-Horizontal Plate Modes Generated Using the Periodic Permanent Magnet EMAT Structure" in this article, travel with a group velocity (this is the velocity of energy or power transport) that depends on the material thickness and the mode frequency. As discussed, for example, in Ref 28, only modes with tightly specified parameters can propagate in any given material and geometry. These modes are divided into two basic classes, symmetric or S-modes and antisymmetric or A-modes; "A" and "S" relate to the symmetry characteristics of the displacements that characterize each mode. Within these two fundamental classes are a large number of discrete modes whose group and phase velocities converge on those of the R-wave (for A_ϕ, S_ϕ) or c_T, the shear velocity, for the higher modes in the limit of large material thickness (which is the same as the high-frequency limit). Figure 10 shows the phase and group velocities for the first four A- and S-modes in steel having a density of 7.85 kg/m^3 and a Poisson's ratio of 0.29. Dispersion curves for other materials may be calculated as described in several places, including Ref 28, or by using the commercial code DISPERSE (Ref 37), which, for example, also allows one to calculate mode displacements and impose non-free-surface BCs. Because the phase and group velocities are a function of the frequency-thickness product (in the literature, this often is expressed as $f \cdot d$ in units of MHz-mm; using the nomenclature of this article, the frequency-thickness product is $f \cdot T$), it is possible to plot a universal set of dispersion curves for each material. When assessing actual uses of plate waves for UNDE, plots of the wave velocities as a function of frequency for each plate or wall thickness of interest are more useful.

The EMATs generate (couple into) guided modes in a manner different from the more common method of using a wedge of low-velocity material (an L-wave velocity in the wedge that is somewhat lower than the shear-wave velocity in the material being evaluated). Wedges couple to surface and guided elastic modes by matching the spatial periodicity of the normal displacement of the incident L-wave to the wavelength of the guided-wave normal displacement; that is, wedges couple into the out-of-plane displacement pattern of the guided wave. The EMATs couple to

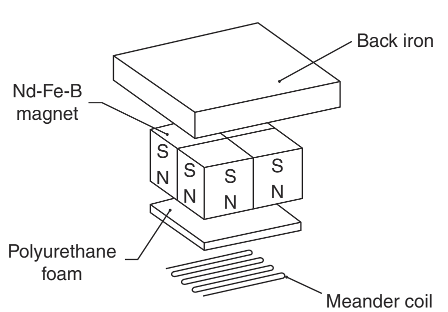

Fig. 9 Schematic of a simple meander coil electromagnetic acoustic transducer that may be used for generating shear-vertical, longitudinal, Rayleigh, and guided waves

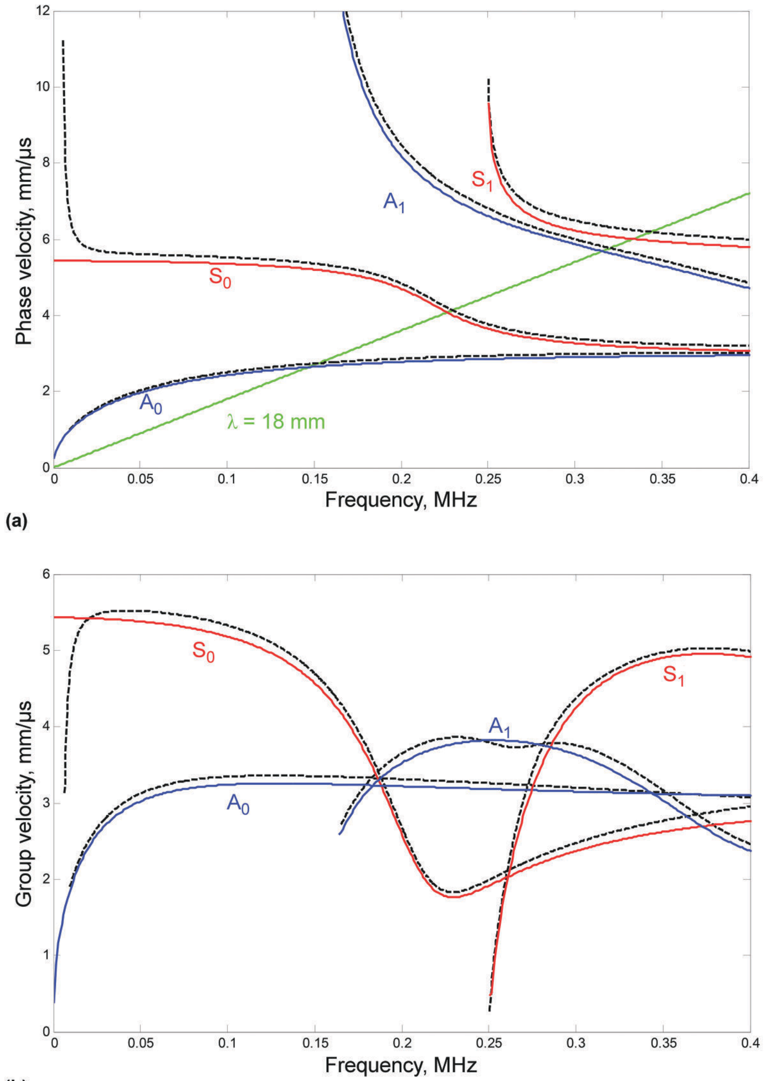

Fig. 10 Dispersion curves for a plate (solid lines) and pipe (dashed lines) of 355 mm (14.0 in.) diameter each of mild steel and each of wall thickness T = 11.1 mm (0.437 in.). Note the more complex dispersion curves for pipes. A larger wall-thickness-to-diameter ratio produces increasingly more complex pipe dispersion curves. This material is to be evaluated using a meander coil of wire spacing D = 9.00 mm (0.354 in.). As is evident in Fig. 11, the value of $\pi T/D = 2\pi T/\lambda = 3.87$ places this operating point at reasonable admittance values for several modes. The T-coil tone burst frequency will determine the mode(s) that are excited (recall that a tone burst actually consists of a range of frequencies). As the pipe wall-thickness-to-diameter ratio decreases, the dashed curves approach their corresponding solid curves.

guided elastic modes by matching the wavelength of the excitation force, which is the period of the MC being used in the EMAT, to the wavelength of the desired guided mode, which is given by $\Lambda = V_p/f$, where f is the T-coil current frequency (the tone burst frequency), and Λ is the wavelength of the guided-mode in-plane surface displacement for a perpendicular bias field (any given MC cannot couple into any desired guided mode; see subsequent discussion). This is the wavelength of the guided mode, which, in general for a free surface, arises from the superposition of at most six partial waves. (These characterize shear displacements, that is, particle motion perpendicular to the propagation direction, and displacements parallel to the propagation direction.) Guided waves also may be generated using a bias field parallel to the surface; in this case, coupling is to the out-of-plane displacements. The dispersion curve is the same for field perpendicular and field parallel cases, but the wave admittances (defined later) are different as shown in Fig. 11.

If the bias magnetic field is at an arbitrary angle with respect to the surface normal, surface excitation will consist of both in-plane (due to the normal field component) and out-of-plane displacements. As noted, there is a different wave admittance associated with each of these displacements; this article deals only with the more common and usually more easily implemented case of a normal magnetic field (in-plane excitation displacements that are coupled to orthogonal, out-of-plane wave-mode displacements through Poisson's ratio).

To relate the previous discussion to a real-world case, consider the guided modes that may be generated by an 18 mm (0.7 in.) period MC (D = 9 mm, or 0.354 in.) in a steel plate of thickness T = 11.1 mm (0.437 in.) and a 355 mm (14 in.) diameter pipe having the same wall thickness. Possible modes are given by the intersection of the line of slope 18 mm with the various modes shown in the dispersion curves in Fig. 10, where solid lines are for the plate and dashed lines are for the pipe. For clarity, Fig. 10 shows only the n = 0 and n = 1 modes up to 0.4 MHz. The efficiency with which these various wave modes are

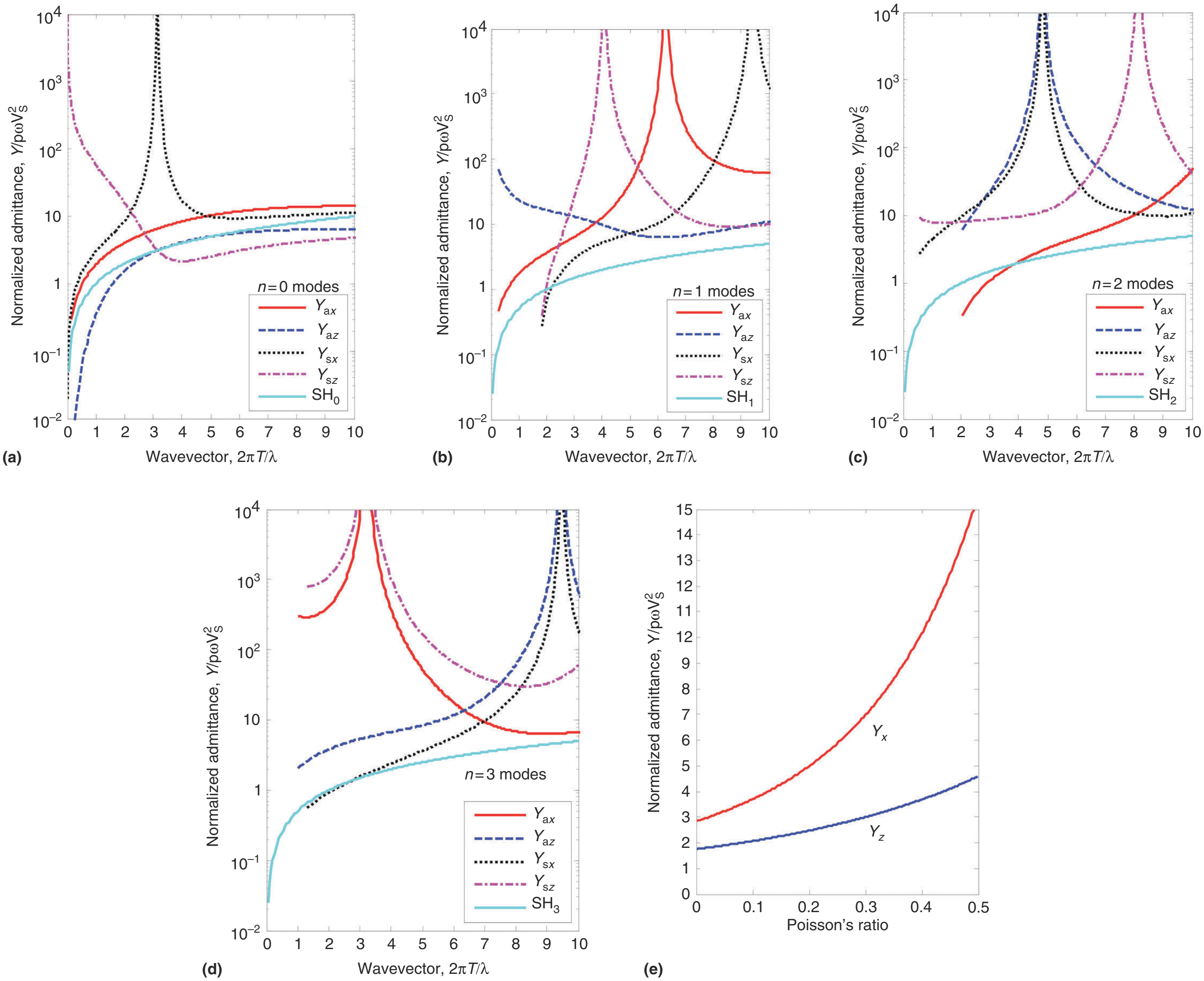

Fig. 11 In (a) through (d), T is the plate thickness, and $\lambda = 2D$ is the wavelength of the excitation force. (a) Normalized admittances for the n = 0 symmetric and antisymmetric Lamb modes and the SH_0 mode. (b) Normalized admittances for the n = 1 symmetric and antisymmetric Lamb modes and the SH_1 mode. (c) Normalized admittances for the n = 2 symmetric and antisymmetric Lamb modes and the SH_2 mode. (d) Normalized admittances for the n = 3 symmetric and antisymmetric Lamb modes and the SH_3 mode. (e) Normalized Rayleigh wave admittances as a function of Poisson's ratio

generated is determined by combinations of the wave admittances given in Fig. 11. Intersection of the wavelength line with the various phase velocity curves (the surface displacement pattern is characterized by the wave phase velocity) determines the frequency of the modes that can be excited with this MC. The relative magnitude of the coupling to these modes is determined by combinations of mode admittances that define the transfer impedance of this MC for the respective modes. (Combinations of admittances for the different modes are given, for example, in Ref 12, 13, 15, 21, and 23.) The T-coil tone burst frequency selects the actual mode(s) that are excited. The admittance curves in Fig. 11(a–e) have been calculated from expressions given in Ref 23. Note that there are errors in some of the admittance curves previously calculated, such as those published in Ref 46; the curves in Ref 23 are the same as those shown in Fig. 11.

In Fig. 11, the subscript "a" designates an antisymmetric mode, and "s" designates a symmetric mode. The parameters "x" and "z" designate the displacement components using the coordinate system shown in Fig. 1. Thus, in Fig. 11(a), Y_{ax} is the admittance for the $n = 0$ antisymmetric mode for a displacement in the x-direction (parallel to the wave propagation direction). For example, based on Ref 21, these quantities combine to give the intrinsic transfer impedance, Z_{TI}, of the $n = 0$ antisymmetric Lamb mode, where N is the number of wavelengths in the T- and R-coils (here assumed to be identical), K is a geometrical factor for the T- and R-MC (they are each near unity), ϕ is the phase angle between the x- and z-components of the particular mode displacement, W is the width of the T- and R-coils (also assumed to be identical), and θ is the angle that B_o makes with the surface:

$$Z_{TI} = 2B_o^2N^2K^2\omega^2W \cdot \{\mathrm{M}(n=0)\},$$
$$\text{with } \{\} \text{ the magnitude of } \mathrm{M}(n=0)$$
$$= \sin\theta/[Y_{xo}]^{0.5} - \exp(j\phi)\cdot\cos\theta/[Y_{zo}]^{0.5}$$

The images in Fig. 11 show the normalized admittance curves for the $n = 0$, 1, 2, and 3 symmetric and antisymmetric guided waves for the first four SH-guided-wave modes and for Rayleigh waves. The range of modes shown in Fig. 11 is approximately the largest that is likely to be needed for guided-wave measurements; these admittance curves are much more difficult to calculate than the dispersion curves shown in Fig. 10. As described in detail in Ref 12 and 23 and outlined in Ref 21, combinations of wave admittances are used to calculate the transfer impedance, insertion loss, and other excitation-efficiency-related parameters for these modes. As shown in Fig. 11(e), the Rayleigh wave admittance is only a function of Poisson's ratio. The relationship between the Rayleigh velocity and Poisson's ratio has been described elsewhere (Ref 46). Except for beryllium, the Poisson's ratio for metals ranges from 0.25 to 0.40, with most at approximately 0.3. The admittance parameters in Fig. 11 and various guided-wave dispersion curves, such as the ones shown in Fig. 10, are needed for designing EMAT meander coils for guided-wave measurements. As noted previously, dispersion curves may be calculated as described in the literature. To have the largest possible received signals, it is very important to pick modes that have a small admittance. (The transfer impedance for any mode is proportional to combinations of the inverse of various wave admittances shown in Fig. 11.) In useful commercial systems where temporal averaging usually must be avoided, one should design for normalized admittances as shown in Fig. 11 to be less than 10. See the section "Additional Comments Related to All Types of Guided Modes" in this article for further discussion of wave admittance calculations.

Shear-Horizontal Wave Generation in Materials that Exhibit Magnetostriction. This is a special case of EMAT elastic-wave generation worthy of mention when discussing EMATs. Magnetoelastic coupling, which includes MS, is the change in the size of magnetic domains when a material is subjected to an applied magnetic field, either static or dynamic. In some materials that exhibit MS, this change in material dimension can occur at high frequency and hence can serve as a means of generating elastic-wave modes useful for UNDE. For the case considered here, the magnetic field is changing at a high frequency (the frequency of the elastic wave being generated). Thus, by its nature, MS excitation in metals, like the Lorentz force, is confined to the material skin depth. Although the physics of this coupling to the elastic body is much more complex and very different from the Lorentz force mechanism, it is discussed here because the transducer configuration and measurement instrumentation essentially is identical to that of a Lorentz force EMAT system that uses a PEM to establish the bias magnetic field. Like the Lorentz force EMAT, the magnetostrictive EMAT uses a combination of an RF magnetic field and a biasing magnetic field to produce elastic displacements at the frequency of the coil current that generates the high-frequency magnetic field. (In a Lorentz force EMAT, it is the external dynamic magnetic field associated with the coil current that produces the induced surface current, which, in turn, gives rise to the Lorentz force.) For MS materials, however, the coupling forces are both different and more complex; for example, the peak MS displacement is approximately parallel to the exciting magnetic field but, in general, not parallel to the bias magnetic field. One example of this complexity and the difference between MS generation and Lorentz force coupling is shown in Fig. 12. One practical use of magnetostrictive SH-guided-wave generation is shown in Fig. 13 (Ref 25).

EMAT Displacement Profiles and Radiation Patterns

Although they may appear to be primarily of academic interest, EMAT displacement profiles and elastic displacement radiation profiles are of extreme practical importance, just as they are for PETs; they must be taken into account in every application of EMATs or, for that matter, any ultrasound generator.

For bulk wave generation, the Lorentz force model and the various specific EMAT input parameters may be used to calculate the displacement field generated by an EMAT and the resulting radiation patterns (sometimes referred to as transducer beam spread). The easiest real EMAT configuration to calculate is for the spiral coil EMAT shown in Fig. 3 (b). References 14 and 19 have provided solutions to this problem, in both cases using the vector potential in the metal given by Ref 47 and 48. Both sets of authors also have compared calculated results with measurements where good quantitative agreement is obtained. Other cases, although similar in principle, require a great deal more analytical and numerical work (Ref 16, 17).

The previously referenced calculations and measurements as well as the calculations and measurements of EMAT radiation patterns given subsequently provide ample evidence that there exists (or could be developed if ever needed) an excellent quantitative understanding (at least within the limitations of the Lorentz force elastic driving mechanism) of any magnet-coil configuration that may be considered for use as a T-EMAT. One interesting

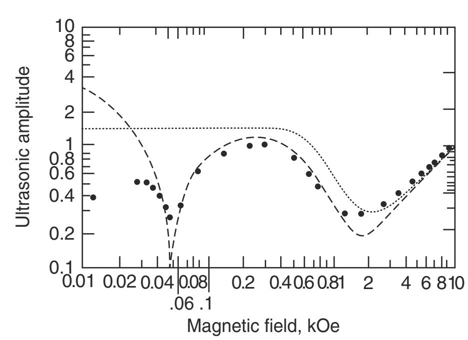

Fig. 12 Magnetic field dependence of the amplitude of the first antisymmetric Lamb mode generated by a tangential field meander coil electromagnetic acoustic transducer in steel (a hot rolled iron plate). The solid broken line is a theoretical prediction based on the measured magnetostrictive (MS) properties, and the dotted line is a theoretical prediction based on a first-principles model for grain rotation contributions to MS. At a bias magnetic field above approximately 3 kOe = 0.3 Tesla, the Lorentz force elastic coupling mechanism dominates. Note that MS coupling peaks at approximately 0.3 kOe, a field that is remarkably easy to generate using a pulsed electromagnet (PEM). Note that a PEM often is required to produce a magnetic field that is accurately parallel to the surface, a condition that is essential in order to achieve significant magnetoelastic coupling in many materials exhibiting MS. Adapted from Ref 12, 15

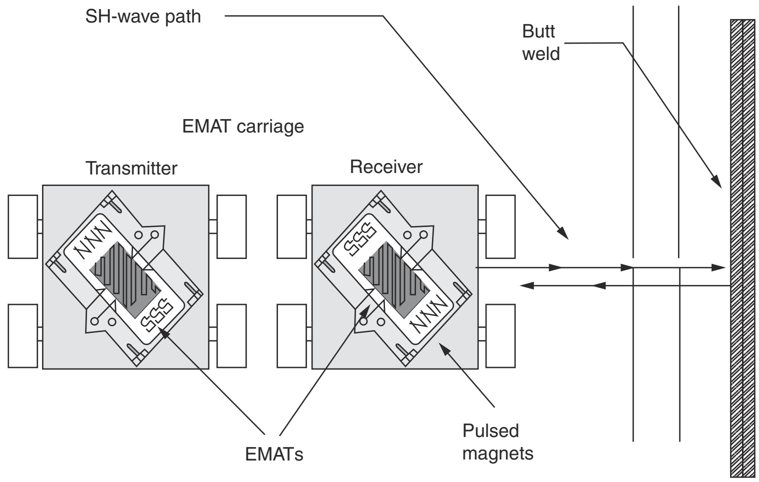

Fig. 13 Pulsed electromagnet and meander coil (MC) structure that is useful for generating shear-horizontal (SH) waves by magnetostriction. Pulsed magnets are used to provide a biasing magnetic field accurately parallel to the metal surface. The angle between this bias field and the radio-frequency (RF) magnetic field produced by a current through the MC is chosen to provide maximum transducer efficiency and is determined by the magnetic properties of the steel. The SH-wave propagation direction is parallel to the RF magnetic field produced by the MC. EMAT, electromagnetic acoustic transducer. Source: Ref 24, 25

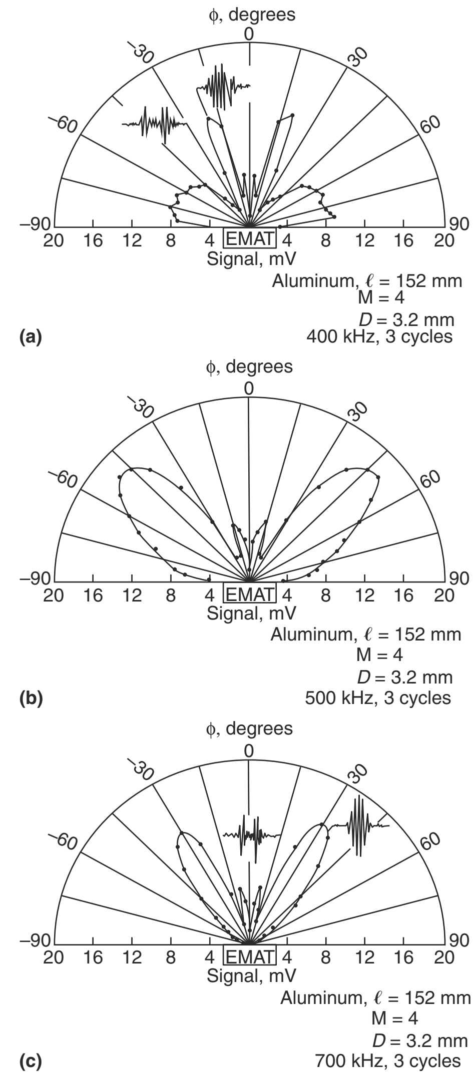

Fig. 14 The shear-horizontal wave directivity or radiation pattern of a periodic permanent magnet shear-horizontal electromagnetic acoustic transducer (EMAT) for (a) 400, (b) 500, and (c) 700 kHz. Adapted from Ref 18

aspect of this ability to calculate an EMAT response very accurately (but one that has yet to be completely exploited) is the possibility of developing an EMAT that could serve as a transfer standard for introducing a known, highly reproducible elastic displacement or displacement profile into a metal. This is especially true for the generation and detection of bulk shear and longitudinal waves but almost certainly could be applied successfully to guided modes.

To summarize work that has been done related to calculating EMAT displacement profiles, the Lorentz force model has been used (Ref 16, 17) to calculate the surface traction (the force that generates the elastic displacements) for different spatial distributions of the current and magnetic field. This work develops the basic equations needed to calculate the surface traction for all three of the basic EMAT types shown in Fig. 6 that have been used with nonmagnetic metals, including PPM and meander coil EMAT structures. In many cases, the formalism presented in Ref 16 and 17 also provides a description of several aspects of magnetic metals. The work of several authors provides beam profiles (radiation patterns) for bulk L- and S-wave propagation. Calculating beam profiles for guided-wave modes is a more complex problem and one that has yet to be done for EMATs. However, beam spread calculations and measurements have been performed for PET-generated guided waves. The most extensive work has been reported in Ref 49, with some information on guided-wave beam spread also given in Ref 50. Reference 49 shows a five-period apodized Lamb wave MC-like polyvinylidene fluoride transducer with a width of approximately 20 MC line separations (approximately 25 mm, or 1 in.) to have a half-amplitude beam width of approximately 25 mm at a distance of 50 mm (2 in.) from the center of the source, with little additional increase in beam width after traveling a distance of over 150 mm (6 in.). Although this case does not relate directly to guided waves generated by EMATs, it does demonstrate that guided-wave beam spread should not be a major sensitivity issue when the transducer width is 10 to 20 times the line spacing and the length is approximately 10 or more times the MC line spacing. These guidelines are consistent with the parameters of most transmit meander coil EMATs in the published literature. It is anticipated that beam spread calculations will be available for meander coil EMATs in the near future. Note that these guidelines do not relate to R-meander coil EMATs, which may be of any length and width consistent with obtaining adequate signal-to-noise ratio (SNR); normally, R-meander coil EMATs will have the same line separation as their related T-meander coil.

The information in Ref 17, and especially that in Fig. 6 to 14 of that paper, is of great value when trying to understand the details of wave propagation from PPM and meander coil EMAT structures as well as how these waves may be received (detected). In particular, reading Ref 16 and 17 is highly recommended before designing/building any practical EMAT, even if one does not contemplate actually doing the specific calculations described therein. Also of great value are calculations (or measurements) of the far-field radiation patterns of EMATs. The reader should note that the far-field distance for guided-wave EMATs, although not yet calculated directly, should depend on the MC width, the number of wavelengths in the MC, the particular mode being considered, and whether the MC has any apodization. Based on experience, the near field probably extends ten or more plate thicknesses beyond the end of the MC being used to generate the guided wave.

Figure 14 shows the beam spread or radiation pattern for a two-period (M = 4) PPM shear-horizontal EMAT similar to the one shown in Fig. 7 at three excitation frequencies: 400, 500, and 700 kHz. The SH surface wave ($\phi = 90°$) is between 400 and 500 kHz. Note the prominent main lobe beams at 500 and 700 kHz. The solid lines in Fig. 14 are measured beam displacement and not calculated results (Ref 18). These radiation patterns are qualitatively similar to those calculated for a six-wavelength-long PPM shear-horizontal EMAT shown in Fig. 24 of Ref 17; the main lobe in that figure is much narrower than the measured response shown in Fig. 14, because the EMAT in their calculations is 3 times longer (and hence generates a beam with smaller divergence). Using a measurement setup described in Ref 18, it is relatively easy to measure the beam characteristics of any bulk wave generated by any EMAT or other transducer, provided the receiving EMAT is chosen to be sensitive to the elastic mode being generated by the transducer under evaluation. Such measurements can be an important step in understanding the details of signals obtained in EMAT measurements.

Additional Comments Related to All Types of Guided Modes

The EMATs have found very widespread use for generating surface and guided waves in metals. The physics of surface- and guided-mode propagation has been described in many places; useful references are Ref 6, 7, 28, and 51. Summarizing descriptions that have been published in many places, no single plane wave can satisfy the free surface BC for waves propagating parallel to the surface of either a half-space or plate. For these cases, one uses a superposition of waves. A surface wave requires the superposition of two waves, one each for the longitudinal and shear displacement components. For a plate, two longitudinal and four shear waves are necessary to satisfy the stress-free BCs at both surfaces. These various wave combinations usually are referred to as partial waves. The situation is more complex for surfaces that are not stress free, such as occurs in coated materials or laminated structures; in many cases, these calculations must be performed numerically. One approach, called DISPERSE, was developed and then continuously improved by Imperial College, London. DISPERSE also provides displacement profiles for the various modes. A version of limited capability is available online. Other approaches to calculating the properties of guided waves also have been developed.

For a half-space, the solution is a Rayleigh wave (R-wave) composed of two partial waves, both decaying with depth and propagating parallel to the surface. For a plate, the partial-wave solution separates into two parts: the first part consists of two shear waves representing displacements that are both parallel to the surface and perpendicular to the propagation direction (these are the SH-plate modes), and the second part consists of two shear waves and two longitudinal waves polarized in the sagittal (x-z) plane and propagating in the x-direction (these directions are as defined in Fig. 1). In plates, these partial waves give rise to the symmetric and antisymmetric Lamb modes.

Exciting any of these surface or guided waves requires periodic excitation forces that match the phase conditions required for coupling into the particular wave mode. Guided and surface waves can be excited with exactly the same EMAT structures mentioned earlier to generate bulk SH- (the periodic permanent magnet EMAT), bulk SV-, and bulk L-waves (the meander coil EMAT). The transfer impedances, however, are very different from the bulk wave cases because the displacements being generated are quite different. For surface- and guided-wave modes, analytical expressions are simpler when written in terms of wave admittances, the inverse of impedances. Using the normal mode formalism (developed for very different purposes) in Ref 52 to 54, Ref 23 calculates the surface displacement of a Lamb wave generated by an MC. From the point of view of exciting guided waves using EMATs, the most relevant parameters calculated by Ref 12, 15, 23, and others are the various wave-mode admittances, Y_M (where M designates the wave mode, $n = 0$, 1, etc.), which depend on the material properties and the specific coil and magnet configuration that is used. These admittances, which also depend on the direction of the excitation current relative to the applied magnetic field, were plotted in Fig. 11.

Many details related to calculating transfer impedances for bulk, surface, and guided waves are given in several places, including Ref 1 to 8 and 12 to 24. Information in the various admittance curves in Fig. 11 and knowledge of the specific dispersion curve (such as the one shown in Fig. 10) for the material structure under study are used to estimate the signal strength that can be expected from an EMAT measurement. Generally, the normalized admittance as shown in Fig. 11 must be less than ten for that mode to be excited with sufficient amplitude to be useful for measurements within an industrial/commercial environment. (Obviously, this number also depends on the T-coil current and the SNR of the EMAT receiver section.)

Making the Transition from Successful Calculations to a Working EMAT System

The following is one possible approach to selecting or designing an EMAT for a guided-wave application. This sample discussion is a generalization of a case previously published in Ref 55 for the assessment of corrosion at pipe supports:

- Calculate or otherwise obtain a dispersion curve for the object to be evaluated. For this example, Fig. 10 shows the dispersion curve for the first four Lamb modes in a mild steel plate and pipe of nominal wall thickness 11.1 mm (0.437 in.) and a pipe diameter of 355 mm (14 in.). The measurement objective is to assess that portion of the pipe over a pipe support for wall loss (a reduction in wall thickness). Based on a model described in Ref 55, a useful Lamb mode must have a substantial group velocity dispersion (this means a strong dependence of group velocity on the pipe wall thickness). One also requires a wave mode having sufficiently small group velocity dispersion that it can travel almost around the pipe circumference. Inspection of the phase velocity curves in Fig. 10 shows that the S_0 mode has a large dispersion at approximately 225 kHz. Also shown in this figure is a line of slope 18 mm (0.71 in.) intersecting the dispersion curve at 225 kHz. Thus, both the T- and R-coils should have a wire spacing of 9 mm (0.354 in.). (The T- and R-coils do not otherwise need to be identical.) The group velocity dispersion is small enough that adequate signals were received after the S_0 mode traveled counterclockwise, as illustrated in Fig. 15, through the region of wall reduction. One follows a similar procedure in selecting Lamb modes for other purposes, such as defect detection, where it is necessary to have knowledge of how effectively a particular defect may scatter or mode convert an incident Lamb mode. This is the subject of many papers, such as Ref 56.
- The EMAT configuration must be such that a change in arrival time of the S_0 mode can be measured when the EMATs are scanned axially from a position of having no pipe support corrosion to one having corrosion. The setup used in Ref 55 and shown pictorially in Fig. 15 is commonly employed for guided-wave measurements on pipes. The T-EMAT normally generates guided waves traveling in both circumferential directions. In this case, the clockwise wave travels in nominally clean pipe, while the counterclockwise wave travels through the pipe support region where, if present, it will encounter corrosion. This approach has proven useful for the assessment of corrosion under pipe support plates and, more generally, for monitoring and even measuring the thickness of plates and pipes.

Assembling a Useful EMAT Measurement System—Magnets, Electronics, and Signal Acquisition/Analysis Considerations

Magnet Considerations. Electromagnets (EMs), pulsed electromagnets (PEMs), and

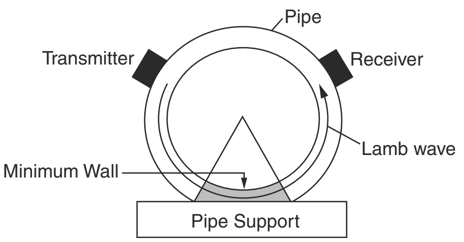

Fig. 15 Basic electromagnetic acoustic transducer for generating guided waves traveling circumferentially in a pipe. Adapted from Ref 55

permanent magnets (PMs) each have been used in building various types of EMATs and EMAT systems. The most widely used and often the most convenient magnets are PMs. The design and use of EMs for a few different types of EMATs has been discussed briefly in Ref 20 to 22. The design and use of PEMs for providing the bias field for EMATs has been discussed in Ref 24 and 57, which also briefly describe the factors influencing the design of PEMs in general. For a detailed description of permanent magnets, the reader is referred to Ref 58 and the literature and services provided by manufacturers, fabricators, and distributors of PM material. Many references throughout this article also contain descriptions of PMs and how they are used for EMAT measurements. Because of their widespread use in EMAT systems, a brief summary of some of the basic characteristics of PMs as they relate to EMATs is given subsequently.

The magnetic field at the end of a PM depends on the length-to-diameter ratio of the PM (in Fig. 3, this is L_M/D_M; the length is measured in the direction of magnetization), the PM material, and the magnetic circuit. In an open magnetic circuit (this means that essentially no other magnetic material is in the vicinity of the PM, a situation similar to that shown for the EMAT in Fig. 3), for $(L_M/D_M) > 1$ for rare earth PMs made of samarium-cobalt alloys, the magnetic field at the end of the PM will be approximately two-thirds of the residual induction. (See Ref 58 for definitions of the magnetic terms used here, as well as for a good description of designing magnetic circuits using PMs.) This same statement applies for $(L_M/D_M) > 2$ for Nd-Fe-B PMs. Prior to the use of PMs containing significant amounts of rare earth materials, PMs were commonly made from Alnico. When placed in an open magnetic circuit similar to the one in Fig. 3, $L_M/D_M > 10$ is necessary to achieve a field at the magnet end that is approximately two-thirds of the residual induction. Currently, the only practical advantage of Alnico PMs in EMAT fabrication seems to be their ability to operate above 500 °C (930 °F) without cooling. (The maximum acceptable operating temperature depends to some extent on the other materials in the magnetic circuit, that is, on the operating point of the magnet in the magnetic circuit.) Under most practical circumstances, Nd-Fe-B PMs can operate up to 80 to 100 °C (175 to 210 °F), and various compositions of samarium-cobalt PMs can operate up to 220 °C (430 °F). Alnico and samarium-cobalt PMs have considerably greater radiation resistance than Nd-Fe-B PMs.

Although electromagnets have not been widely used in commercial applications of EMATs, there are several cases where their features have proven to be very desirable. Often, they should at least be considered for some EMAT designs. Because an EM has the advantage that the field may be turned off, using an EM may be a safety consideration, especially when large EMATs must be used on or near large volumes of magnetic metal. It should be noted, however, that mechanical approaches have been used to permit the magnetic field in a magnetic plate coupled to a PM to be switched on and off between large and small values. One old and common use of this is in the fabrication of magnetic attachment devices.

The PEMs, another means of providing a bias magnetic field, were mentioned with respect to the EMAT measurement configuration shown in Fig. 13. Probably the first use of pulsed-field EMATs was reported in Ref 57. There have been other successful applications of pulsed electromagnet EMATs since then (Ref 24, 25). In most cases, the pulse current and pulse power required for a pulsed electromagnet EMAT are modest, typically under 100 A at 100 V with an on time of 0.1 to 1 ms and a duty cycle of under 3%. Although PEMs normally are used when an EMAT design requires a field parallel to the surface, they also may be used for normal-field EMATs if the large voltage induced in the R-coil is managed when the T- and R-coils are in close proximity. Not included as a PEM is the self-field EMAT, which requires a pulsed current in excess of a few thousand amperes that usually requires a voltage pulse in excess of 1000 V.

The PEMs basically are a coil with a core of thin laminated magnetic material, such as a special type of iron or air. Because the field requirements are modest, an air core often is the most convenient for use with MS materials. Note, however, that an air-core PEM requires a significantly larger magnet current. If a magnetic/conducting core is used, lamination is needed so that eddy-current generation does not seriously limit the rate at which fields can increase or decrease, as well as possibly to minimize heat generation in the core. Pulsed electromagnet EMATs are used primarily when relatively low fields (less than 0.1 Tesla) and/or low repetition rates or duty cycle (less than 100 Hz or 1%) are acceptable. One main advantage of PEMs is the ease of generating a magnetic field parallel to the metal surface in either magnetic or nonmagnetic metals, because the transient nature of the field means that it takes time to penetrate into the metal; hence, for short coil current on times, the field is confined to the surface.

In any EMAT system, a magnetic field is required to receive elastic displacement signals (although some research applications have used an optical laser interferometer as a surface displacement sensor, Ref 59); thus, in a PEM system, either a separate source of receiver bias field must be used (provided by either another PEM or an appropriately designed PM) or the pulsed field must be present and not changing rapidly in time if the same PEM is to serve as both generator and receiver of elastic displacements.

Very Basic EMAT Measurement System. Figure 16 is a schematic of the front end of a general EMAT system for either pulse-echo or pitch-catch measurements.

Figure 17(a) shows a typical six-cycle half-bridge output voltage across the inductive load. Depending on the load inductance, the current in the T-coil will look something like the current waveform shown in Fig. 17(b). Transformers T_1 and T_2 normally are not used with the direct-drive EMAT current sources described briefly in the next section.

EMAT Transmit Electronics. It is common practice for EMAT system developers to use commercial pulsed power systems and components. These systems also may incorporate functions such as R-coil signal amplification and EMAT signal processing needed for doing EMAT measurements. Some information on electronics that may be useful when developing EMAT solutions to NDE problems is available in the many patents related to EMATs that have been published over the past 40 years. Note that information in unexpired patents can be proprietary. Searches of U.S. patents are easy to perform and may be downloaded at no cost.

In general, solid-state electronic power sources such as linear power amplifiers, full-bridge direct-drive, and half-bridge direct-drive configurations are used in EMAT systems. As illustrated in Fig. 17, direct drive refers to applying a positive EMAT T-coil excitation voltage very rapidly to the T-coil, allowing the current to build up in the T-coil inductor, switching off this excitation voltage, waiting some time for the current to decrease substantially to zero, applying a negative T-coil excitation voltage, allowing the current to build up in the T-coil inductor, switching off this excitation voltage, waiting some time for the current to decrease substantially to zero, and repeating this process for the number of cycles desired for the tone burst (TB). Full- and half-bridge, direct-drive current sources are much easier and lower cost to design and build than linear amplifiers, but they have the potential disadvantage of generating an excitation current with considerable odd-harmonic content. Low-cost, low-voltage (under 150 V peak) direct-drive systems may be designed that are capable of providing peak currents in the range of 30 to 100 A into many practical T-EMAT coils. The practical upper frequency for these drivers usually is determined by the T-coil inductance. Using a direct-drive system, a 1 to 20 cycle TB of excitation power at frequencies in the range of 0.05 to 5.0 MHz with a duty factor of 0.1 to 1% may be produced rather easily. Generally, this entire range of performance specifications is not required for any given EMAT application. However, achieving such an ambitious design goal is possible, although it may be time-consuming.

It should be noted that these EMAT drivers are quite different from those used in most PET systems. (The exception is for high-

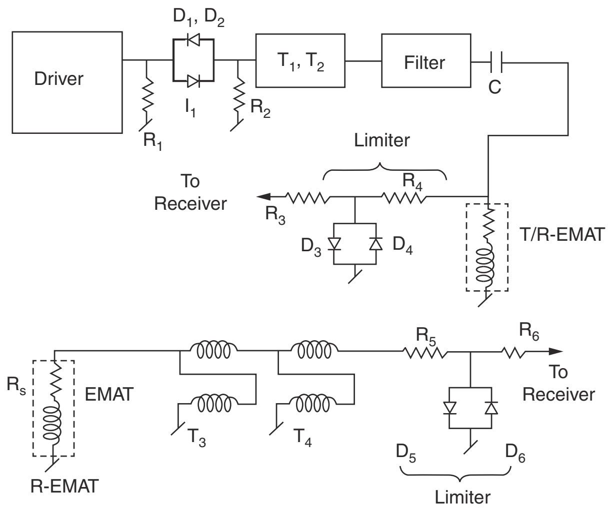

Fig. 16 Schematic representation of pulse-echo (PE) (upper image) and pitch-catch (PC) (lower image) electromagnetic acoustic transducer (EMAT) systems. Normally, separate T- and R-coils are used even for the PE configuration; in this case, a thin strip or wire R-coil (less than a skin depth of conductor thickness) may be placed beneath the larger-wire-diameter T-coil. Functions of the various system components are as follows: (i) The combination of resistors R_1 and R_2 and isolator I_1, which is represented by diodes D_1 and D_2, ensure that, even at low output voltage, the EMAT driver has a load and a direct current path to ground for the isolator. (ii) Isolator I_1 minimizes the influence of coupling of any low-voltage ringing in the driver output to the R-coil. Typically, isolators consist of a large number of series (to keep the capacitance small) and parallel (so that a large current can be managed by small-signal, low-capacitance switching diodes) combinations of back-to-back diodes to provide adequate isolation between the driver and the receiver electronics. There also are other solid-state devices that can substitute for diodes and thus, in the PE configuration, to the sensitive receiver input. (iii) T_1 and T_2 are impedance-matching transformers to maximize power transfer from the driver to the T-coil. (Frequently, only one transformer is needed, but a larger EMAT system bandwidth, if needed, often can be achieved using multiple impedance-matching transformers.) (iv) If harmonic content in the EMAT current must be minimized (such as may be useful for some types of signal processing), a filter, either low pass or high pass, as appropriate, is sometimes useful (but keep in mind that many EMATs are themselves a very good filter). (v) When very long EMAT current tone bursts are used, series tuning of the EMAT may improve the overall system signal-to-noise ratio by increasing the current available from the driver. (vi) Resistors R_3 and R_4 and a sequence of voltage-limiting back-to-back diodes, represented by D_3 and D_4, serve to limit the voltage at the EMAT receiver amplifier input. (vii) Transformers T_3 and T_4 are receiver amplifier input impedance-matching transformers. (Transmission line transformers placed in series are sometimes used when the EMAT system bandwidth must be maximized; otherwise, a single transformer with a voltage stepup of as much as 50:1 may be used. The maximum useful voltage stepup is determined by the R-coil resistance, R_S, and the preamplifier input resistance, R_A. Refer to Fig. 2.)

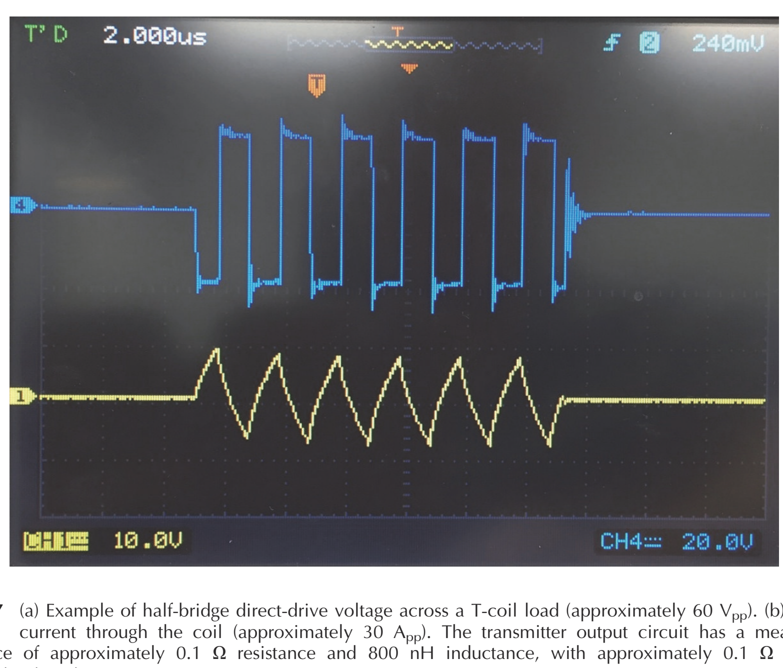

Fig. 17 (a) Example of half-bridge direct-drive voltage across a T-coil load (approximately 60 V_{pp}). (b) Resulting current through the coil (approximately 30 A_{pp}). The transmitter output circuit has a meander coil impedance of approximately 0.1 Ω resistance and 800 nH inductance, with approximately 0.1 Ω additional transmit circuit resistance.

power, low-frequency PET systems where high output current may be needed to charge the transducer capacitance to a high voltage in a fraction of the RF period.) The objective of the EMAT driver is to pump current through the coil. When using linear amplifiers, the driver output impedance often is considerably larger than the EMAT coil impedance, so some form of impedance matching, represented by transformers T_1 and T_2 in Fig. 16, is used to make the best possible use of the power available from the driver. Because the current used to excite an EMAT can reach several hundred amperes, a matching transformer may require ferrite cores having a large cross-sectional area, sometimes in excess of 100 mm^2 (0.16 $in.^2$). Another approach is to design the EMAT coil so that it matches the EMAT driver that is being used. This usually is practical for coils such as those shown in Fig. 4(a, b) but often not practical for MCs. Typically, impedance-matching transformers are not used in direct-drive EMAT systems, but they almost always are used with linear power amplifiers.

EMAT Receive Electronics. Using an EMAT as a receiver is a very different circuit function from using it as a transmitter. Whereas commercial electronic solutions to obtaining an acceptable EMAT driver, the source of the EMAT current, are either easy to fabricate (especially for currents less than 20 to 40 A peak) or may be purchased, optimized EMAT receive electronics often require considerable analysis by the engineer responsible for developing the EMAT application if optimum EMAT system performance is to be achieved. Some EMAT systems have addressed these receiver issues when used with a defined set of R-EMATs. Following is a discussion about optimizing receiver performance when separate T- and R-coils are used. Based on the authors' experience, this should be the EMAT system design goal whenever possible, even if the T- and R-coils are placed above or adjacent to each other. For guided-wave modes, it is important to select a receiver coil optimized for the mode (the type of displacement and its wavelength) one wishes to receive. This normally will be a receiver coil that has the same wire spacing as the transmitter. However, the receiver coil can be and often should be narrower and even shorter than the transmitter coil. (T-coils usually need to minimize beam spread and hence may be wider and longer than is necessary or desirable for R-coils.) Also note that apodization usually reduces the sensitivity of an R-coil unless special signal processing is used, something that usually is very challenging when working with dispersive waves.

The displacement amplitude available at the R-coil is determined by its position in relation to the T-coil, the physical characteristics of the T-coil, the T-coil driver, and the properties of the elastic medium. The length of R-coil wire that is adjacent to the metal surface (the wire that is effective in receiving an EMAT signal) can, in some cases, be made longer than the T-coil wire. For example, a receive MC may have multiple wires (turns) within each wavelength; this increases the R-coil wire length. Because of its much larger inductance, a multiwire T-MC can be a disadvantage, because this may require a disproportionately larger driver voltage to obtain the same T-coil current. (Although impedance matching may compensate for some of this increase in inductance, the normal result is to have an overall decrease in the potential SNR in such an EMAT system.) However, so long as the R-coil is not a long distance (say, less than a meter) from the receiver electronics, at typical EMAT operating frequencies (below 5 MHz), impedance-matching transformers are at least as effective at increasing the receiver SNR as is a multiturn R-coil. Sometimes it is desirable to place small R-coil impedance-matching transformers in a soft iron enclosure to shield the transformer core from external magnetic fields. Because R-coil voltages are very small, careful attention to grounding, shielding, and guarding throughout the receiver circuit usually pays large dividends.

In the pulse-echo version of the EMAT system shown in Fig. 16, the receiver coil has a direct electrical connection to the driver even when the driver is not supplying current to the EMAT coil. Thus, some form of isolation, represented by I_1 and various back-to-back, voltage-limiting diodes in Fig. 16, is needed between the receiver input and driver output. Figure 16 shows these components placed at the driver output and the receiver input, but they also may be placed in other parts of the EMAT circuit, such as I_1 after the filter and, if used, after the tuning capacitor. The resistors R_3 and R_4, which should be somewhat larger than the EMAT impedance, aid in recovery and protection of the receiver electronics. If a long cable is used between the EMAT drive and receive electronics (not a recommended approach; at a minimum, there should be some portion of the receive electronics near the R-coil), then the isolator and impedance-matching transformers (for both T- and R-coils) should be as close as possible to the EMAT. Resistors R_3 to R_6 are noise sources in the receiver circuit; hence, they should be as small as possible, consistent with providing adequate isolation and overload protection.

Using half-bridge or full-bridge driver configurations (Ref 60, 61), one generates a quasi-square voltage pulse (Fig. 17) having the dominant frequency required for the EMAT current. It is quite obvious that this is not the time dependence assumed in writing the various equations that are solved, for example, to obtain a solution to Maxwell's equation or the expressions and graphs presented previously in the section "Essential Features of Practical EMATs when Used as Transmitters and Receivers" in this article. Under most practical circumstances, square-wave voltage excitation works just fine (one notable exception is with resonance EMAT systems), partly because the EMAT itself often acts like a narrowband filter. This is especially true for the EMAT structures shown in Fig. 6, because they are inherently narrowband devices. The various normal-beam shear-horizontal EMAT structures discussed in this article are broadband receiving devices, but the NBSH T-coil is a frequency-dependent load to its driver; thus, at constant voltage excitation, the T-coil current is frequency dependent. Also, although the transfer impedance sometimes may be frequency independent, the R-coil output voltage is proportional to frequency. If the EMAT user is concerned about direct drive of the EMAT generating unwanted harmonic content in the elastic wave, then an appropriate filter, as indicated in Fig. 16, can be placed in the drive circuit. However, keep in mind that such a filter may reduce the excitation current available to the T-coil and significantly lengthen the TB (which increases the so-called dead time for the EMAT system). In general, the T-EMAT circuit should be critically or slightly underdamped to avoid a long receiver electronics recovery time.

In Fig. 16, the tuning capacitor, C, can be useful if very long TBs are used, but otherwise it should be avoided (again, one exception to this may be in resonant EMAT systems). In pulsed systems, this capacitor should be chosen so that it forms a slightly underdamped or critically damped circuit with the T-EMAT circuit resistance, inductance, and series and shunt capacitances. When used, it is best to place C close to the T-EMAT coil. Also, the voltage across the capacitor can substantially exceed the driver output voltage. In all cases, remember that the cables connecting the T- and R-coils to their various electronics have both inductance and capacitance that will influence system performance. There are many useful tips on working with RF circuits in Ref 62. In particular, there is a description of narrowband matching between a transmitter and an inductive load (e.g., an EMAT).

In the pulse-echo configuration, unless separate coils are used, the receiver is connected directly to the EMAT driver during the time the excitation current is applied to the T-coil. (Even when separate coils are used, the R-coil will have a large voltage induced in it by the T-coil current.) Because the voltage across the EMAT easily can reach many hundreds of volts (the transient voltage can be as much as twice the driver output voltage), it is easy to damage the sensitive electronics in the receiver circuit. Diodes D_3 to D_6 are there to protect the receive electronics. Resistor R_3 in the limiter circuit should be a few times larger than the EMAT impedance to minimize shunting of the drive current around the EMAT when operating as a single-coil pulse-echo measurement system (not recommended practice). Resistors R_3 and R_4 in combination with their associated back-to-back diodes are there to protect the sensitive receiver electronics. During the on time of the T-pulse, the back-to-back diodes (there are other solid-state devices that may replace these diodes) have a resistance that is small compared to R_3, R_4, R_5, or R_6, so the diode-resistor combinations function as voltage dividers to protect the receiver electronics from high-voltage damage. One reason for using series and parallel combinations of diodes is to minimize capacitive coupling between the driver and EMAT when the driver is off. However, because these resistors add noise to the receiver circuit, their values should be as small as possible, consistent with providing the required protection. Depending on the sensitivity of the preamplifier to overload damage, R_4 and R_6 may not be needed. The input impedance, Z_R, of the receiver preamplifier should be at least a few times larger than the largest value in the preamp circuit (R_3, R_4, R_5, or R_6, as appropriate) to avoid significant signal loss due to this voltage divider. As described subsequently, the resistances in the receiver circuit are significant noise sources. It can be a challenging task to balance all of the competing factors, especially if, as usually is the case, receiver impedance-matching transformers T_3 and T_4 are used. (Note that often only one transformer is required.) In addition to diodes, there are other solid-state components with a resistance that is voltage dependent.

The most important system factors to consider when using EMATs as receivers are to select low-noise preamplifiers and then to implement good impedance matching between the R-coil and this preamplifier. This requires matching the EMAT coil resistance, R_S, to the amplifier input resistance, R_A. Referring to Fig. 2, $Z_A = R_A - jX_A$ and normally $X_A = 1/\omega C_A$, where C_A is the capacitance at the receiver input. The R-coil resistance sometimes is as small as a fraction of an Ohm, while the noise equivalent input resistance of a low-noise preamplifier usually is in the range of 30 to 100 Ω. Without proper impedance matching, this mismatch can result in an enormous loss of SNR, an extremely important parameter in any EMAT system. Usually, one may not think of a 30 Ω input resistance amplifier as introducing any significant issues when the source has a 1 Ω resistance. However, for small received signals and without using impedance matching, noise from the amplifier input resistance can easily dominate the system noise behavior. The best SNR is achieved when the source resistance, R_S, is as small as possible and yet dominates the system noise. This can be achieved, or at least approximated, through impedance matching.

Sometimes, the aforementioned considerations may dictate altering the EMAT system diagram shown in Fig. 16. Usually, two approaches are available. The first, not shown in Fig. 16 and usually not recommended, is to use an active (electronic) switch to connect/disconnect the R-coil to/from the receiver electronics. Just before initiating the current pulse through the T-coil, the switch connecting the R-coil to the preamplifier is opened so there is a high impedance between the EMAT drive circuit and receiver electronics. Normally, the main problem in achieving good isolation of the preamplifier from the T-coil current pulse is capacitive coupling between the T- and R-coils. Note that even when the T- and R-coils are not in close physical proximity to each other, they each are often closely coupled to ground, and various coaxial cables often connect the T- and R-coils. Active isolation of the T- and R-coils from the receive electronics during the T-coil excitation time sometimes may be useful, even when the recommended practice of separate T- and R-coils is implemented. After the drive current has returned to zero and the stored energy in the T- and R-coil inductances has dissipated, the switch is closed to connect the R-coil to the preamplifier. This allows for optimum matching of the R-coil to the preamplifier and enables one to obtain the smallest possible electronic noise in the receiver circuit. The second and recommended approach is to use a separate R-coil and no active isolation. If one uses a printed circuit R-coil or an R-coil made of fine wire, the R-coil may be placed beneath the T-coil without adding much additional coil and magnet liftoff or screening of the fields generated by the T-coil. (Of course, in this case, there can be a large capacitive coupling between the two coils.) Using an R-coil placed near the T-coil still leaves one with a large voltage induced in the R-coil. This almost always is best managed by the isolation approaches outlined in Fig. 16; in the authors' experience, using an active switch seldom is the best approach to achieving the largest SNR or electronic system overload recovery time. In practice, switching transients usually are difficult to manage.

Broadband impedance-matching transformers for the frequency range requirements of most EMAT systems often are of the transmission line type and are available commercially. Because currents in the EMAT receiver circuit are small if a well-designed approach to isolation is used, a receiver impedance-matching transformer will not require ferrite cores of large cross-sectional area. Areas in the range of 1 to 5 mm^2 (0.002 to 0.008 in.^{2}) normally are used; note, though, that a large overload pulse such as may occur in a system with poor isolation can saturate the core of a small R-coil impedance-matching transformer. Ferrite components in EMAT circuits can saturate (and hence make the ferrite useless) if they are in close proximity to any magnet; ferrite cores in impedance-matching transformers usually must not be subjected to magnetic fields larger than several Gauss or mTesla. Note, though, that a magnetic field shielding enclosure may be used.

Although it is common to use small-diameter wire or printed circuit traces for EMAT receiver coils, the resistance of the rest of the receiver circuit before the impedance-matching transformers should be made as small as possible to minimize the source noise resistance. A larger receiver bandwidth can be achieved when the distance between the R-coil and the matching transformer is minimized, because this minimizes the effective source capacitance. It also is important to shield the R-coil and any connecting wires from stray electromagnetic pickup, because this noise also may appear directly as a source of noise. When the T-coil is in close proximity to the R-coil, it too should be shielded from stray electromagnetic pickup so this does not couple into the receiver circuit. Sometimes, a thin metal foil (thinner than one skin depth) is placed in front of the EMAT coils (especially between the R-coil and the metal surface); this shield should be grounded to the EMAT frame or to the material being assessed using a very tight mechanical or, preferably, a soldered connection that is as short as possible. In a very noisy electrical environment, it may be beneficial to use triaxial cables and differential amplifiers to minimize common mode noise; the outer shield is used as a guard (Ref 63, 64). (One good approach is to perform an Internet search for "guards and shielding to protect small signal integrity." This is more likely to yield results of greatest use for a specific issue.)

Noise Considerations Related to R-EMAT Electronics. A combination of random electronic and coherent acoustic noise ultimately limits the SNR performance of any EMAT system. (This assumes that coupling of stray electromagnetic fields into the receiver circuit has been eliminated by careful attention to grounding and guarding of critical portions of the receiver circuit, a task that frequently is very difficult to achieve.)

Random electronic noise always will be present. The mean squared noise voltage in volts due to a resistance of R Ohms, V_N^2, is given by $V_N^2 = 4kTR\Delta f$, where the Boltzmann constant is $k = 1.38 \cdot 10^{-23}$ J/K, T_K is the temperature in Kelvin, and Δf is the system electronic noise bandwidth in Hertz. As a practical example, take a bandwidth of 1 MHz and use an R-coil having an RF resistance of 5 Ω. (This is higher than most wire-wound or printed circuit EMAT coils that are near a permanent magnet and a metal surface.) At T_K = 300 K, this gives a noise voltage of V_N = 0.3 μV_{rms}. Assuming the low-noise preamplifier has an equivalent input noise resistance of 40 Ω (a value of approximately 0.8 nV/$\sqrt{\text{Hz}}$ and which is available in several commercial integrated circuit amplifiers using the same parameters), this will contribute a noise voltage of V_{NR} = 0.8 μV_{rms}. A 1-to-9 impedance-matching transformer (a voltage transformation of 1 to 3) will give a total noise voltage for this R-coil at the amplifier input of approximately 1.2 μV_{rms}. (The resultant total noise voltage, V_{NT}, is the square root of the sum of the squared noise voltages or $V_{NT} = (V_N^2 + V^2_{NR})^{0.5}$, where V_N is the amplifier noise and V_{NR} is the resistor noise voltage.) Thus, a 1 μV_{rms} signal from the EMAT coil gives a 3 μV_{rms} signal at the amplifier input for an input SNR of 2.5. Without the transformer, the SNR is (1.0/0.85) = 1.2. Just using a matching transformer doubled the system SNR. Some EMATs have a source resistance as small as 0.1 Ω; impedance matching frequently will achieve an overall increase in SNR of 20 or more. This is the difference between a signal that cannot be viewed, without temporal averaging, on an oscilloscope and one that may be used directly for various UNDE tasks.

Based on the discussion in the section "Some EMAT Configurations for Bulk Elastic-Wave Generation—An Introduction to the Behavior of Practical EMATs" in this article, the intrinsic transfer impedance of an EMAT similar to that shown in Fig. 5, where the coil has ten active turns/centimeter in an area of 1.0 cm^2 (0.16 in.^{2}), is approximately 4.8 μΩ for steel. (For a pole area of 2.5 cm^2, or 0.39 in.^{2}, the magnetic field in the test block is approximately 1.1 Tesla.) Therefore, a T-coil current of 30 A peak (approximately 21 A_{rms}) gives an R-coil output voltage of 101 μV_{rms} or, for the aforementioned case, an ideal SNR of approximately 126, not taking into account signal reduction due to magnet and coil liftoff. In practice, this particular coil inductance and resistance are both too large to obtain much advantage by impedance matching. Also, in practice, this SNR likely will be smaller due to RF pick-up noise (see the subsequent discussion). One also should note that the intrinsic transfer impedance of typical meander coil EMAT systems often is under 0.1 μΩ.

One factor that easily can nullify any effort at impedance matching is electromagnetic pickup. The RF fields in the EMAT frequency operating range are everywhere (e.g., think of AM broadcast signals). If good practice with respect to shielding and grounding has been exercised, it usually is possible to reduce the general pick-up noise in a receiver circuit to an additional noise contribution in the range of 0.3 to 3.0 μV_{rms} referred-to input of the preamplifier. From the previous noise and signal estimates, it is clear that good shielding and grounding methods are essential for meaningful and reproducible EMAT measurements. This is especially true for meander coil EMATs where the transfer impedance frequently is less than 0.1 μΩ and the source impedance is in the range of 0.1 to 1.0 Ω. In this case, impedance matching is essential to optimizing the performance of the EMAT system. A good measure of the overall system noise is obtained when the EMAT system is operating, but there is no current in the T-coil.

Coherent acoustic noise also can be a problem in EMAT systems; this is much more difficult to estimate and, if present, to eliminate. In EMAT systems, this type of noise has three main sources: grain scattering and/or multiple reflections in the material being studied; elastic waves generated in the EMAT magnet and case by the transmitter current that, at a later time, induce a voltage in the R-coil (clearly, this contribution is present only when the T- and R-coils share the same magnet); and elastic energy generated by one pulse of current in the T-coil being propagated and reflected within the material under study and returning to the R-coil as a "ghost" signal that forms part of a subsequent received signal. Spatial averaging is a signal-processing method that can be used to reduce coherent noise due to grain scattering and multiple reflections (Ref 65, 66). Temporal averaging of electronic signals, commonly used to improve the SNR, does not reduce coherent acoustic noise. The presence of coherent noise is easily deduced by performing temporal averaging of the EMAT signal for an increasingly larger number of averages. If, at some point, the SNR does not improve with the number of averages, then there are noise sources that have a coherent relationship with the EMAT signal. Frequently, this coherent relationship is due to the acoustic noise mentioned earlier.

The system electronic noise can, of course, be reduced by decreasing the signal bandwidth. Although this usually is not of great use when a half-cycle or single-cycle excitation pulse is used, it can be of considerable benefit when multicycle TBs are used to excite an EMAT for applications such as guided-wave measurements. Longer TBs permit a smaller-system bandwidth to be used. There are both analog and digital methods for reducing the signal bandwidth (Ref 67). Digital methods offer the greatest flexibility, but analog methods can be an advantage if the data-acquisition system lacks sufficient dynamic range, because filtering before digitization can prevent noise from saturating the digitizer.

Signal Analysis Techniques. An extensive discussion of the many very useful signal analysis methods that are available when working with EMAT signals will not be undertaken here. The following mentions some general and widely available methods that generally prove useful.

Temporal averaging is the coherent summing of consecutive waveforms that are nominally identical except for noise. Because the signal adds coherently and the noise adds randomly, temporal averaging improves the SNR of the averaged waveform. The SNR improvement is proportional to the square root of the number of times the signal with random noise is summed. Many digitizing oscilloscopes have an averaging feature, and signal-averaging software is available in many standard signal-processing software packages (Ref 67).

Spatial averaging requires that the receiving transducer be moved a small distance with respect to the transmitting transducer between each received waveform acquisition. In this way, elastic-wave scattering from grains and other internal structure is made somewhat random in a small region near the R-coil where, it is assumed, the signal otherwise would be reasonably constant. Spatial averaging is accomplished by acquiring signals for a number of closely spaced EMAT positions. These signals must be added by shifting each in time by an appropriate amount that is related to the distance moved.

In many EMAT applications, it is required to know the time between two received signals or the time from the start of the transmit signal to the received signal with high accuracy or resolution (these are not the same). The time between two signals can be determined very accurately by calculating the cross-correlation function (CCF) of the two signals (Ref 68). For example, suppose that two receivers separated by some distance are used to obtain signals produced by the same Lamb wave traveling in a plate; this can be accomplished using two MCs separated by a known distance, such as illustrated in Fig. 4. The Lamb wave travel time between the two receivers can be obtained by calculating the CCF of the two signals. Many points in each signal are involved in this calculation. Using interpolation methods, the resolution available in this travel-time calculation can be greater than the digitization interval used in acquiring the waveform. The time difference between two signals also may be obtained from the phase difference of the fast Fourier transform of the two signals (Ref 69).

Easy-to-Assemble, Basic EMAT System. Most EMAT systems designed for a specific NDE application are likely to be complex; these either can be purchased directly from equipment suppliers, assembled using commercial components, or assembled from a combination of commercially available components and individually designed ones. Note that both separate EMAT system components and practical complete EMAT systems are commercially available. It is possible (likely) that a commercial system may need to be modified to enable a development engineer to explore the full range of EMAT system parameters she/he may wish to evaluate. Some companies may be reluctant to disclose proprietary company information to an equipment supplier in order to provide the information needed by the equipment vendor to make the necessary modifications to their equipment. If such disclosures must be avoided, the methods outlined in this article and the basic system described here may offer the design engineer the needed flexibility in determining the EMAT system parameters that are important for their particular application. Note, however, that this usually is not the most time-efficient approach.

Figure 18 is one example of a flexible, useful, basic EMAT system that may be used with any of the permanent magnet EMATs discussed in this article. It is adaptable for use with any bulk or guided-wave approach that employs separate T- and R-coils. As such, it illustrates all the basics of an EMAT measurement system. If these coils are in close proximity, special considerations related to overload and recovery of the receive electronics likely will be required. Reference 62 is useful for selecting and, if needed, fabricating impedance-matching transformers for both the T- and R-coils. Signal-processing digital oscilloscopes are widely available for a modest cost. Although data acquisition using a digital oscilloscope is too slow for commercial applications, they can be used to digitize, time

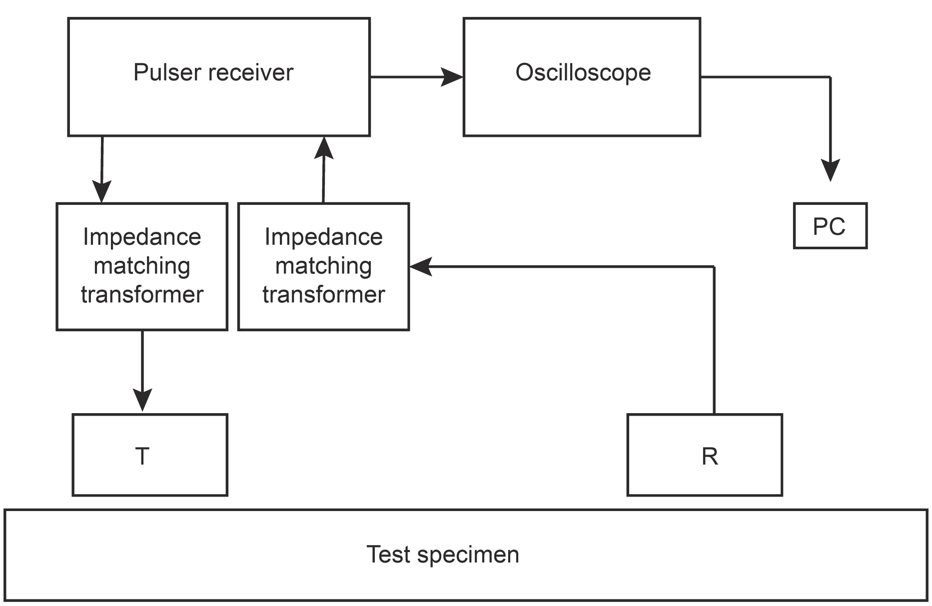

Fig. 18 Basic electromagnetic acoustic transducer system